This article has been accepted for publication in a future issue of this journal, but has not been fully edited. Content may change prior to final publication. Citation information: DOI 10.1109/TWC.2016.2527650, IEEE Transactions on Wireless Communications

Modeling and Analysis of Opportunistic Beamforming for Poisson Wireless Networks

Tharaka Samarasinghe, *Member, IEEE,* Hazer Inaltekin, *Member, IEEE,* and Jamie S. Evans, *Member, IEEE*

***Abstract*—This paper introduces a model to study both single tier and multi-tier wireless communication systems consisting of a multitude of wireless access points (AP), and operating according to the classical opportunistic beamforming framework. The AP locations in the proposed network model are determined by using planar Poisson point processes. The extreme value distribution of signal-to-interference-plus-noise-ratio (SINR) on a beam is of fundamental importance for obtaining performance bounds for such an opportunistic communication system. Two tight distribution approximation results are provided for the distribution of maximum SINR on a beam, which is hard to obtain due to correlation structure of the underlying inter-AP interference field, using key tools from stochastic geometry. These approximations hold for general path loss models that satisfy some mild conditions. Simulations and numerical evaluations are presented to validate the results, to provide further insights into the derived approximate maximum beam SINR distributions, and to illustrate the utility of these approximations in obtaining performance bounds for opportunistic communication systems having multiple interfering APs. In particular, key performance measures such as beam outage probability and ergodic aggregate data rate of an AP are derived by utilizing the approximated distributions.**

***Index Terms*—Communication systems, Data communication, MIMO systems, Opportunistic beamforming, Stochastic processes**

I. Introduction

Opportunistic beamforming (OBF) is an important adaptive signaling technique that utilizes multiuser diversity and varying channel conditions to extract the full multiplexing gain available in vector broadcast channels [1]–[20]. The main advantages of OBF are threefold. It attains the sum-rate capacity with full channel state information (CSI) to a first order for large numbers of mobile users (MU) in the network [1]. Secondly, its operation only requires partial CSI in the form of signal-to-interference-plus-noise ratios (SINR). Finally, OBF is easy to implement, which makes it a practical communication scheme. It has been also shown that OBF is an asymptotically feedback optimal transmission strategy [5]. This paper introduces an analytical framework to study single tier and multi-tier OBF wireless communication networks consisting of multiple interfering wireless access points (AP) by modeling their locations using spatial Poisson point processes (PPP).

For single AP communication systems, the well known system model of opportunistic communication along multiple orthonormal beams was first introduced by Sharif and Hassibi in [1]. In this work, the authors considered a multi-antenna vector broadcast channel over which an AP communicates with N MUs that are equidistant from the serving AP. The orthogonal beams are randomly generated, and each beam is allocated to the MU having the highest SINR on that beam. Most of the existing works on OBF are based on this model having homogeneous and equidistant MUs from the AP [1]–[7].

On the other hand, heterogeneity among MUs was also considered in previous works such as [8] and [9], where each MU has its own deterministic location dependent path loss value, *i.e.*, the MUs are no longer equidistant from the home AP. In [8], heterogeneous MUs are grouped into a finite number of MU classes, and the asymptotic throughput scaling behavior of the resulting system is analyzed. In [9], the authors focused on the sum rate and the individual throughput scaling while simultaneously maintaining fairness among the MUs. Recently, the model was further improved in [10] by introducing random MU locations that are governed by a spatial PPP and assigning a random path loss value to each MU. The authors in [10] mainly focused on the outage capacity of the network by taking the random MU locations into account. All of the above papers consider OBF for only *single* AP communication systems by ignoring inter-AP interference among potentially interfering APs.

Different from these previous works, we take a step further in this paper to model and analyze OBF communication systems consisting of *multiple* interfering APs (multi-AP) by using spatial PPPs to model the AP locations. Also, being different than the conventional structure introduced in [1], the MUs communicating with a particular AP are not equidistant from it. This introduces heterogeneity among the MUs as well. The proposed model allows us to study OBF for both single tier and K-tier multi-AP communication systems. Similar to [8], [9] and [10], the signal received by an MU in this paper is impaired by both fading and the location dependent path loss. However, unlike [8], [9] and [10], the communication quality at an MU is also degraded by signals transmitted from interfering APs.

Since the MUs are not equidistant from an AP, the path loss values between the MUs and its home AP, which we

This work was supported in part by the Australian Research Council (ARC) under Grant DP-11-0102729, in part by the Scientific and Technological Research Council of Turkey (TUBITAK) under Grant 112E024 and in part by Marie Curie FP7-Reintegration-Grants within the 7th European Community Framework Programme under Grant PCIG10-GA-2011-303713.

T. Samarasinghe is with the Department of Electronic and Telecommunication Engineering, University of Moratuwa, Sri Lanka (e-mail: tharaka@ent.mrt.ac.lk).

H. Inaltekin is with the Department of Electrical and Electronics Engineering, Antalya International University, Turkey (e-mail: hazeri@antalya.edu.tr).

J. S. Evans is with the Department of Electrical and Electronic Engineering, University of Melbourne, Australia (e-mail: jse@unimelb.edu.au).

1536-1276 (c) 2015 IEEE. Personal use is permitted, but republication/redistribution requires IEEE permission. See http://www.ieee.org/publications_standards/publications/rights/index.html for more information.

This article has been accepted for publication in a future issue of this journal, but has not been fully edited. Content may change prior to final publication. Citation information: DOI 10.1109/TWC.2016.2527650, IEEE Transactions on Wireless Communications

call the intra-AP path loss values, are different among the MUs communicating with a particular AP. The intra-AP path loss values are considered to be arbitrary but deterministic positive real numbers. On the other hand, the path loss values between an MU and its interfering APs, which we call the inter-AP path loss values, are random and governed by a path loss model $G(r)$, where r is the distance from the interfering AP. The network is a fully closed-access network, *i.e.*, the MUs communicate only with their respective home APs. For an example, one can consider a multitude of Wi-Fi networks, where each network has its own security measures to prevent unauthorized access.

The related work also includes papers such as [11]–[14] and [21]–[24], that study multiuser MIMO. The main point of difference between the network model introduced in this paper and those introduced in [11]–[14] is that these previous studies consider the AP locations to be known, similar to grid based cellular models, which is in sharp contrast to our random AP locations model. Recent studies indicate that irregular AP locations in communication networks of today resemble to the random Poisson deployment, rather than regular grid based topologies [25], [26]. To this end, [21]–[24] use stochastic geometric approaches to model the AP locations, but their operation is not based on partial CSI, which make them different than this paper. To the best of our knowledge, this is the first paper that considers random AP locations to model multi-AP OBF communication systems and that uses key tools from stochastic geometry to analyze the performance of the resulting wireless communication system.

Transmissions are scheduled to MUs having the highest received SINR on each beam in an OBF communication system. Therefore, the distribution of the maximum SINR on a beam emerges as an important summary statistics for the performance analysis of OBF communication systems. For single AP OBF communication systems, the calculation of the extreme value distribution of SINR on a beam is relatively simple to carry out since the SINR values received by MUs on a particular beam constitute a collection of independent random variables. In particular, for the baseline model of opportunistic communication introduced in [1], the SINR values on a beam turn out to be independent and identically distributed (i.i.d.) random variables among the MUs since they are equidistant from the AP. Hence, the extreme value distribution of SINR on a beam for the system in [1] can be simply obtained by raising the individual beam SINR distributions to the power of N for a communication scenario consisting of N MUs.

However, unlike single AP OBF communication systems such as [8], [9] and [10], the SINR values on a beam for the multi-AP system model considered in this paper are no longer independent among the MUs. They are dependent on the common randomness caused by the point process governing the locations of the interfering APs. This dependency makes it prohibitively hard to derive the exact distribution of the maximum SINR on a beam, and hence, it becomes relatively much more complicated to perform performance analysis for multi-AP OBF communication systems. The heterogeneity among the MUs does further multiply the complexity as it makes the SINR values on a beam non-identically distributed among the MUs.

Towards the resolution of this complication, we provide two tight distribution approximation results. To obtain the first approximation, we assume that the inter-AP interference is independent among the MUs connected to a particular AP. Intuitively, this approximation should give rise to a close match to the actual scenario for APs with large coverage radii since MUs are expected to be further away from each other in this case, and the spatial correlation of inter-AP interference will diminish to zero for large distances [27]. For the second approximation, we assume that the inter-AP interference is perfectly correlated. Intuitively, this approximation should lead to a close match to the actual scenario for APs with small coverage radii since in this case, the MUs are expected to be close to each other, and the spatial correlation of inter-AP interference will increase to one for small distances [27].

We derive analytical expressions for the extreme value distribution of beam SINR values under these approximations for both single tier and multi-tier networks, and illustrate that the proposed distribution approximation results match the realistically simulated distribution of the maximum beam SINR values quite well. The derived expressions hold for general path loss models that satisfy some mild conditions, including the commonly used unbounded path loss model $G(r) = r^{-\alpha}$. Further, we use these approximation results to obtain performance bounds for multi-AP OBF communication systems by focusing on beam outage probabilities and achievable aggregate ergodic data rates of each AP.

The rest of the paper is organized as follows. In Section II, we introduce the system model to analyze multi-AP OBF communication systems. In Section III, we study the distribution of the maximum SINR on a beam and derive analytical distribution approximation results to approximate the distribution of maximum SINR on a beam. In Section IV, we extend our baseline model introduced in Section II for single tier multi-AP OBF wireless networks to K-tier heterogeneous multi-AP OBF wireless networks, with each tier modeling a particular class of networks, similar to macro-cells, pico-cells or femto-cells in a cellular environment. The results analogous to those obtained in Section III for the distribution of maximum SINR on a beam are also obtained for K-tier multi-AP OBF communication systems in Section IV. Note that the intra-AP path loss values are considered to be arbitrary but deterministic, which implies that the MU locations are deterministic. This is done in order to ensure clarity in our main results. However, according to conventional assumptions when stochastic geometry is applied to model wireless networks, both APs and MU locations are assumed to be subject to PPPs, albeit with different intensities. In Section V, we will discuss how the results in this paper can be extended to a scenario where both AP locations and MU locations are random.

To illustrate the applications of our analytical distribution approximation formulas derived for general path loss models as well as to gain further insights, we derive the extreme value distribution for beam SINR levels by using two well known path loss models in Section VI. We provide simulations and

1536-1276 (c) 2015 IEEE. Personal use is permitted, but republication/redistribution requires IEEE permission. See http://www.ieee.org/publications_standards/publications/rights/index.html for more information.

This article has been accepted for publication in a future issue of this journal, but has not been fully edited. Content may change prior to final publication. Citation information: DOI 10.1109/TWC.2016.2527650, IEEE Transactions on Wireless Communications

numerical evaluations in Section VII to validate the results and to discuss the utility of each approximation for getting insights into a realistically simulated OBF communication system. In particular, we demonstrate that when the coverage radius is small, the approximated maximum beam SINR distribution obtained by assuming perfect correlation gives rise to a close match to the actual case in both sparse and dense networks. On the other hand, the approximation result obtained by assuming that the inter-AP interference is independent among the MUs connected to a particular AP performs better for sparse networks when the coverage radius is large. When the coverage radius is large and the network is dense, both approximations do not perform well, and for this particular scenario, we propose using a mix of the two approximations to better approximate the actual case. Finally, we utilize the approximate maximum beam SINR distributions to obtain some important performance measures for multi-AP OBF communication systems such as beam outage probability and ergodic aggregate data rate per AP in Section VII. Section VIII concludes the paper.

II. System Model and Problem Setup

In this section, we will present our system model as an extension of the classical single AP OBF framework with homogeneous MUs [1] to a scenario of heterogeneous MUs and multiple interfering APs. To simplify notations, we focus only on the system model for a single tier network in this section. The extensions to the multi-tier case are given in Section IV. To this end, we consider a wireless network with APs located according to a homogeneous spatial PPP Φ of intensity λ. Each AP is equipped with T transmit antennas and communicates with a multitude of MUs having single receive antennas. The network is assumed to be a *fully closed-access network*. That is, the MUs communicate only with their respective home APs similar to a multitude of Wi-Fi networks, where each network has its own security measures to prevent unauthorized access.

Being different from [1], the MUs communicating with a particular AP are not equidistant from it, which introduces additional heterogeneity among them. Each AP has a circular disk-shaped coverage area of radius D, and we assume that an MU lying outside of the coverage area will not be able to communicate reliably with the AP. This means that each AP and the locations of the MUs that communicate with it can be illustrated by using points lying inside a disk of radius D, where the AP is located at the center of the disk. For a particular realization of AP locations and a selected part of the plane, Fig. 1 gives a graphical illustration of the proposed model for the multi-AP OBF wireless communication network. An inactive MU is an MU outside the coverage region of its home AP. As shown in Fig. 1, an inactive MU may be located inside the coverage area of a neighboring AP, but it cannot receive any data by connecting to the neighboring AP as the network is assumed to be closed access. The same situation also applies to an active MU that is much closer to a neighboring AP compared to its home AP.

The received signal by an MU is impaired by both fading and path loss. We assume that the path loss value between an

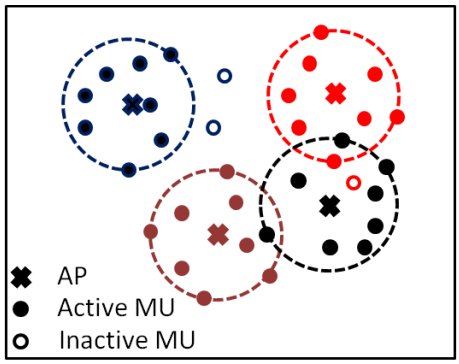

Fig. 1. Part of the plane illustrating AP and MU locations for a particular realization of AP locations.

MU and its home AP is a fixed arbitrary positive real number, and we call this the intra-AP path loss value of the respective MU. Note that the intra-AP path loss values are different among MUs since they are not equidistant from the home AP. On the other hand, the path loss values between an MU and its interfering APs, which we call the inter-AP path loss values, are random and governed by a path loss model $G(r)$, where r is the distance between the MU and an interfering AP. Our path loss model is general in the sense that G can be any function that is continuous, positive and non-increasing as well as satisfying the relation $G(r) = O\left(r^{-\alpha}\right)$ as r grows large for some $\alpha > 2$.[1]

The network operates according to the classical OBF framework [1] as follows. Each AP transmits M, $M \leq T$, different data streams intended for M different MUs. We assume that the origin o belongs to the AP location process Φ and focus on a test AP located at the origin $o \in \Phi$. This assumption does not limit the generality of our results due to Slivnyak's Theorem [28]–[30]. The symbols of the mth stream transmitted from the AP located at the origin are represented by $s_{o,m}$. They are drawn from a zero mean and unit variance *circularly-symmetric complex Gaussian* distribution $\mathcal{CN}(0,1)$, and are sent along the directions of M orthonormal beamforming vectors $\{\boldsymbol{b}_{o,m}\}_{m=1}^{M}$. The overall transmitted signal from the AP located at the origin is given by

$$\boldsymbol{s}_o = \sqrt{P}\sum_{m=1}^{M} \boldsymbol{b}_{o,m} s_{o,m}, \tag{1}$$

where P is the transmit power per beam.

Consider MU i located at $u_i \in C_D$, where C_D represents the disk centered at the origin with a radius D. The MU at u_i communicates with the serving AP located at the origin. Let $\|u_i - y\|$ be the distance between the MU located at u_i and an AP located at $y \in \Phi \setminus \{o\}$, where $\|\cdot\|$ represents the Euclidean norm. The signal received by the MU i at u_i is given by

$$Y_i = \sqrt{g_i}\boldsymbol{h}_{o,u_i}^{\top}\boldsymbol{s}_o + \sum_{y\in\Phi\setminus\{o\}} \sqrt{G(\|u_i - y\|)}\boldsymbol{h}_{y,u_i}^{\top}\boldsymbol{s}_y + Z_i, \tag{2}$$

[1]The variable r in $G(r)$ is actually normalized by a reference distance D_{ref}. For example, in cellular networks, typical distances for D_{ref} are on the order of a kilometer for macro-cells, of hundred meters for pico-/micro-cells and of several meters for femto-cells [26]. r takes the same units as D_{ref}. In the current paper, and in most related other works in the literature, it is assumed that $D_{\text{ref}} = 1$ unit distance. Therefore, both λ and D in this paper can be considered as normalized quantities with respect to the unit distance.

1536-1276 (c) 2015 IEEE. Personal use is permitted, but republication/redistribution requires IEEE permission. See http://www.ieee.org/publications_standards/publications/rights/index.html for more information.

This article has been accepted for publication in a future issue of this journal, but has not been fully edited. Content may change prior to final publication. Citation information: DOI 10.1109/TWC.2016.2527650, IEEE Transactions on Wireless Communications

where g_i is the intra-AP path loss value of MU i, Z_i is the $\mathcal{CN}(0,1)$ additive background noise, $\boldsymbol{h}_{o,u_i}$ is the T-by-1 complex vector containing fading coefficients between the MU at u_i and the AP at the origin. Similarly, $\boldsymbol{h}_{y,u_i}$ is the T-by-1 complex vector containing fading coefficients between the MU at u_i and the AP located at y. We assume that the fading coefficients are i.i.d. random variables drawn from $\mathcal{CN}(0,1)$.

Let $\gamma_{o,u_i,m}$ be the received SINR value at the MU located at u_i, corresponding to beam m transmitted from the home AP. The first term on the right hand side of (2) represents the received useful signal. The second term represents the interference signals from all interfering APs located according to $\Phi \setminus \{o\}$. Thus, $\gamma_{o,u_i,m}$ is given by

$$\gamma_{o,u_i,m} = \frac{g_i X_{o,u_i,m}}{(P)^{-1} + g_i I_o + \sum_{y\in\Phi\setminus\{o\}} G(\|u_i - y\|) I_y}, \quad (3)$$

where $X_{o,u_i,m} = |\boldsymbol{h}_{o,u_i}^{\top}\boldsymbol{b}_{o,m}|^2$, $I_o = \sum_{l=1,l\neq m}^{M} X_{o,u_i,l}$ and $I_y = \sum_{l=1}^{M} X_{y,u_i,l}$. Here, we note that $X_{y,u_i,l} = |\boldsymbol{h}_{y,u_i}^{\top}\boldsymbol{b}_{y,l}|^2$ is the (unnormalized) inter-AP interference power at the MU located at u_i arising from beam l transmitted by the AP located at y. Each MU feeds back its SINR information to its home AP, and the home AP selects the MU with the highest SINR on each beam to maximize the communication rate. Therefore, the instantaneous rate on beam m transmitted from the test AP at the origin (measured in terms of nats/s/Hz) can be written as

$$\text{rate}_m = \log\left(1 + \max_{1\leq i\leq N} \gamma_{o,u_i,m}\right), \quad (4)$$

where N is the number of home MUs within the coverage area of the test AP at the origin.

III. Distribution of the Maximum SINR on a Beam for General Path Loss Models

In the system model we put forward in Section II, the distribution of the maximum SINR on a beam emerges as an important parameter for the network performance analysis. Indeed, the CDF of the maximum beam SINR value provides us with necessary and sufficient statistical characterization of a multi-AP OBF communication system to calculate outage and ergodic data rate capacities of the system. We note that this observation is also correct for the single AP OBF communication systems where the distribution of the beam SINR F was first derived, and then by using the fact that the SINR on a beam is i.i.d. among the MUs, the distribution of the maximum SINR on a beam was simply obtained by raising F to the power of N [10]. The calculation of the extreme value distribution of beam SINR values for multi-AP OBF communication systems becomes strikingly more complicated due to two reasons. Firstly, the MUs are not equidistant from the BS, thus the SINR on a beam is not identically distributed among the MUs. Secondly, due to the correlation structure of the underlying inter-AP interference field, the SINR on a beam is not independent among the MUs either. Below, we first present the steps taken towards obtaining tight bounds on the maximum beam SINR distribution. Then, we elaborate on the performance characterization of multi-AP OBF communication systems further in Section VII by utilizing the derived extreme value distribution approximation results.

When considering the SINR expression in (3) given for a multi-AP OBF communication system, it can be seen that $X_{o,u_i,m}$ is exponentially distributed with unit mean, *i.e.*, $X_{o,u_i,m} \sim \exp(1)$. This means that due to being summations of i.i.d. unit mean exponentially distributed random variables, I_o is distributed according to $\Gamma(M-1,1)$ and I_y is distributed according to $\Gamma(M,1)$, where $\Gamma(k,\theta)$ represents the gamma distribution with shape parameter k and scale parameter θ. By using these observations, we first present the auxiliary result below, where we condition on the locations of the interfering APs and derive the conditional distribution of the SINR on a beam for the MU located at u_i.

Lemma 1: Consider the AP located at the origin $o \in \Phi$, MU i at $u_i \in C_D$. Let $\Phi_o^! = \Phi \setminus \{o\}$ represent the point process governing the locations of the interfering APs. For a given realization of $\Phi_o^!$, the distribution of the SINR on a beam for the MU at u_i and communicating with the AP at o is given by

$$F_{u_i}\left(t|\Phi_o^!\right) = 1 - \frac{\exp\left(\frac{-t}{g_i P}\right)}{(t+1)^{M-1}} \prod_{y\in\Phi_o^!} \tilde{G}_i(t, u_i - y), \quad (5)$$

where

$$\tilde{G}_i(t, u_i - y) = \frac{g_i^M}{\left(g_i + tG(\|u_i - y\|)\right)^M}.$$

Proof: See Appendix A. ∎

Since the SINR values on a beam at different MUs are dependent upon each other through the common randomness caused by the point process governing the locations of the interfering APs, we have first conditioned on the point process of locations of interfering APs in Lemma 1 to remove this dependency. By utilizing this conditional CDF result for individual beams, we can readily obtain an expression for the conditional distribution of the maximum SINR on a beam transmitted from the AP at $o \in \Phi$, which can be written as

$$F^{\star}\left(t|\Phi_o^!\right) = \prod_{i=1}^{N} F_{u_i}\left(t|\Phi_o^!\right).$$

Hence, the unconditional maximum beam SINR distribution can be written as

$$F^{\star}(t) = \mathsf{E}_{\Phi_o^!}\left[\prod_{i=1}^{N}\left[1 - \frac{\exp\left(\frac{-t}{g_i P}\right)}{(t+1)^{M-1}} \prod_{y\in\Phi_o^!} \tilde{G}_i(t, u_i - y)\right]\right]. \quad (6)$$

The dependency among individual beam SINR values makes it prohibitively hard to obtain an analytical expression for the expectation in (6), and therefore we cannot derive a closed form result for the maximum SINR on a beam. Towards the resolution of this complication, we formally present two approximations for the distribution of the maximum SINR on a beam by using key tools from stochastic geometry below.

1536-1276 (c) 2015 IEEE. Personal use is permitted, but republication/redistribution requires IEEE permission. See http://www.ieee.org/publications_standards/publications/rights/index.html for more information.

This article has been accepted for publication in a future issue of this journal, but has not been fully edited. Content may change prior to final publication. Citation information: DOI 10.1109/TWC.2016.2527650, IEEE Transactions on Wireless Communications

A. Independent Inter-AP Interference Approximation

We will obtain our first approximation on the maximum beam SINR distribution by assuming that inter-AP interference random variables are independent among the MUs connected to a particular AP. This means that each MU located in the circular coverage area C_D observes an independent realization of the point process that governs the locations of interfering APs. This assumption makes the beam SINR values among the MUs connected to the same home AP independent, which, in turn, leads to an easier computation of the maximum SINR distribution on a beam. Thus, under the assumption of independent inter-AP interference values, $F^{\star}(t)$ in (6) can be approximated as

$$F^{\star}(t) \approx F^{\star}_{\mathrm{ind}}(t) \triangleq \prod_{i=1}^{N}\left[1-\frac{\exp\left(\frac{-t}{g_i P}\right)}{(t+1)^{M-1}}\mathsf{E}_{\Phi_o^!}\left[\prod_{y\in\Phi_o^!}\tilde{G}_i(t,u_i-y)\right]\right]. \quad (7)$$

This means that we can obtain the distribution of the maximum beam SINR by first obtaining the beam SINR distributions of the MUs connected to the AP at the origin, and then considering the product of these individual beam SINR distributions. These ideas are formally presented through the following theorem, and intuitively, this approximation should give rise to a close match to the actual scenario for APs having large coverage radii since MUs are expected to be further away from each other in this case, and the spatial correlation coefficient of inter-AP interference will diminish to zero for large distances [27].

Theorem 1: Under the independent inter-AP interference assumption, the CDF of the maximum SINR on a beam transmitted from an AP communicating with N MUs having intra-AP path loss values $\{g_i\}_{i=1}^{N}$ can be approximated by

$$F^{\star}_{\mathrm{ind}}(t)=\prod_{i=1}^{N}\left[1-\frac{\exp\left(-q_{1,i}(t)\right)}{(t+1)^{M-1}}\right],$$

where

$$q_{1,i}(t)=\frac{t}{g_i P}+\sum_{m=0}^{M-1}\int_0^{\infty}\frac{\pi\lambda t g_i^m G(\sqrt{r})}{\left(tG(\sqrt{r})+g_i\right)^{m+1}}dr.$$

Proof: See Appendix A. ∎

If we consider the expression obtained for $F^{\star}_{\mathrm{ind}}$ more closely, the first term of the function $q_{i,1}$ represents the effect of the background noise on the maximum beam SINR distribution, and the second term represents the effect of inter-AP interference on the maximum beam SINR distribution. On the other hand, the $1/(t+1)^{M-1}$ term arises due to intra-AP interference. For example, if $M=1$, *i.e.*, single rank transmission, this term vanishes since using a single beam eliminates intra-AP interference among the MUs connected to the same home AP. Through the following corollary, we will further simplify the result in Theorem 1 to a scenario where the N MUs communicating with the AP at the origin are equidistant from it. In other words, it is assumed that all N MUs receive signals from their home AP at the same average power. In the literature associated with OBF, this is the most common assumption made for the modeling of MU locations [1]–[7].

Corollary 1: Under the independent inter-AP interference assumption, the CDF of the maximum SINR on a beam transmitted from an AP communicating with N equidistant MUs having the same intra-AP path loss value g can be approximated by $F^{\star}_{\mathrm{ind}}(t)=\left[1-\frac{\exp\left(-q_1(t)\right)}{(t+1)^{M-1}}\right]^N$, where

$$q_1(t)=\frac{t}{gP}+\sum_{m=0}^{M-1}\int_0^{\infty}\frac{\pi\lambda t g^m G(\sqrt{r})}{\left(tG(\sqrt{r})+g\right)^{m+1}}dr.$$

Next, we will provide another approximation for the CDF of the maximum SINR on a beam transmitted from an AP.

B. Perfectly Correlated Inter-AP Interference Approximation

We will obtain our second approximation on the maximum beam SINR distribution by assuming that inter-AP interference random variables are perfectly correlated among the MUs connected to the same home AP.[2] This assumption makes the conditional beam SINR values (conditioned on the interfering AP locations) among the MUs connected to the same home AP independent, which again leads to an easier computation of the maximum SINR distribution on a beam. Under this assumption, by using the stationarity property of $\Phi_o^!$, $F^{\star}(t)$ in (6) can be approximated as

$$F^{\star}(t)\approx F^{\star}_{\mathrm{cor}}(t) \triangleq \mathsf{E}_{\Phi_o^!}\left[\prod_{i=1}^{N}\left(1-\frac{\exp\left(\frac{-t}{g_i P}\right)}{(t+1)^{M-1}}\prod_{y\in\Phi_o^!}\tilde{G}_i(t,y)\right)\right], \quad (8)$$

where we average over the location process of the interfering APs after considering the product of the individual beam SINR CDFs of the MUs to obtain our second approximation on the maximum beam SINR distribution. Intuitively, this approximation is expected to give rise to a close match to the actual scenario for APs having small coverage radii since the MUs are expected to be close to each other in this case and the spatial correlation coefficient of inter-AP interference will increase to one for small distances [27]. We will first present an auxiliary result that we will use to derive the above approximation.

Lemma 2: For any collection of real numbers $a_1,\ldots,a_N$, we have

$$\prod_{i=1}^{N}(1-a_i)=\sum_{\mathcal{S}\subseteq\{1,\ldots,N\}}(-1)^{|\mathcal{S}|}\prod_{i\in\mathcal{S}}a_i,$$

where we take $\prod_{i\in\mathcal{S}}a_i=1$ if $\mathcal{S}=\phi$.
The lemma can be easily proven by using induction, and therefore, omitted in the paper. As an example for the use of Lemma 2, we get $(1-a_1)(1-a_2)(1-a_3)=1-a_1-a_2-a_3+a_1a_2+a_1a_3+a_2a_3-a_1a_2a_3$ for $N=3$. Also note that if $a_1=a_2=\ldots=a_N=a$, Lemma 2 simplifies to the well known binomial expansion.

[2]The term representing inter-AP interference consists of both path loss values and fading coefficients. The correlation is with respect to path loss values. The fading coefficients are still considered to be i.i.d. random variables.

1536-1276 (c) 2015 IEEE. Personal use is permitted, but republication/redistribution requires IEEE permission. See http://www.ieee.org/publications_standards/publications/rights/index.html for more information.

This article has been accepted for publication in a future issue of this journal, but has not been fully edited. Content may change prior to final publication. Citation information: DOI 10.1109/TWC.2016.2527650, IEEE Transactions on Wireless Communications

Using the result in Lemma 2, the perfectly correlated inter-AP approximation is formally presented in the following theorem.

Theorem 2: Under the perfectly correlated inter-AP interference assumption, the CDF of the maximum SINR on a beam transmitted from an AP communicating with N MUs having intra-AP path loss values $\{g_i\}_{i=1}^{N}$ can be approximated by

$$F^{\star}_{\mathrm{cor}}(t) = \sum_{\mathcal{S}\subseteq\{1,\ldots,N\}} \frac{(-1)^{|\mathcal{S}|}}{(1+t)^{|\mathcal{S}|(M-1)}} \exp\left(-q_2(t,\mathcal{S})\right),$$

where

$$q_2(t,\mathcal{S}) = \sum_{i\in\mathcal{S}} \frac{t}{g_i P} + \pi\lambda \int_0^{\infty} \left(1 - \prod_{i\in\mathcal{S}} \frac{g_i^M}{\left(g_i + tG(\sqrt{r})\right)^M}\right) dr.$$

Proof: See Appendix A. ∎

Compared to the result in Theorem 1, the result in Theorem 2 is less tractable analytically. Even, numerical evaluation is not straightforward when N is large. Therefore, we resort to the equidistant assumption again, where the AP communicates with N equidistant MUs. If the MUs are equidistant with a common intra-AP path loss value g, (8) can be simplified as

$$F^{\star}_{\mathrm{cor}}(t) \triangleq \mathsf{E}_{\Phi^{!}_o}\left[\left(1 - \frac{\exp\left(\frac{-t}{gP}\right)}{(t+1)^{M-1}} \prod_{y\in\Phi^{!}_o} \frac{g^M}{(g+tG(\|y\|))^M}\right)^N\right].$$

This assumption does not only make the conditional beam SINR values (conditioned on the interfering AP locations) among the MUs connected to the same home AP independent, but also makes them identically distributed. The simplified maximum SINR distribution is formally presented in the following corollary.

Corollary 2: Under the perfectly correlated inter-AP interference assumption, the CDF of the maximum SINR on a beam transmitted from an AP communicating with N equidistant MUs having the same intra-AP path loss value g can be approximated by

$$F^{\star}_{\mathrm{cor}}(t) = 1 + \sum_{i=1}^{N} \frac{\binom{N}{i}(-1)^i \exp\left(-q_{2,i}(t)\right)}{(1+t)^{i(M-1)}},$$

where

$$q_{2,i}(t) = \frac{it}{gP} + \sum_{m=0}^{Mi-1} \int_0^{\infty} \frac{\pi\lambda t g^m G(\sqrt{r})}{\left(tG(\sqrt{r})+g\right)^{m+1}} dr.$$

Proof: See Appendix A. ∎

Note that there is only a subtle difference in the derivations of the two approximations in Theorems 1 and 2 above. In the independent inter-AP interference scenario, we performed averaging over the reduced Palm distribution of the interfering AP locations before calculating the extreme value distribution for beam SINR values, whereas we calculated the conditional extreme value distribution for the beam SINR values first in the perfectly correlated inter-AP interference scenario and then averaged over the reduced Palm distribution of the interfering AP locations to remove conditioning. Further, by focusing on the two simplified expressions in Corollaries 1 and 2, we can observe subtle structural differences between the expressions obtained for the two cases as well. By binomial expansion, $F^{\star}_{\mathrm{ind}}(t)$ in Corollary 1 can be written as

$$F^{\star}_{\mathrm{ind}}(t) = 1 + \sum_{i=1}^{N} \frac{\binom{N}{i}(-1)^i}{(1+t)^{i(M-1)}} \times \exp\left(-\frac{it}{gP} - i\sum_{m=0}^{M-1} \int_0^{\infty} \frac{\pi\lambda t g^m G(\sqrt{r})}{\left(tG(\sqrt{r})+g\right)^{m+1}} dr\right).$$

From a more practical point of view, the analytical structural differences in these two approximation results help us to understand the statistical behavior of maximum beam SINR values for a multi-AP OBF network at the two extreme cases of large and small D. The extreme value distribution of the beam SINR values in the actual scenario is expected to lie in between these two limiting cases, a point which we illustrate in detail numerically in Section VII. We should also note that by direct observation of the results in Theorems 1 and 2, and Corollaries 1 and 2, we can see that the CDF of the maximum SINR on a beam transmitted from an AP goes to one exponentially fast with increasing AP intensity and decreasing intra-AP path loss values.

IV. OBF for Networks with Heterogeneous APs

In this section, we will extend the results obtained for single tier multi-AP OBF wireless communication networks in Section III to a K-tier heterogeneous network, with each tier modeling a particular class of network. Let $\mathcal{K} = \{1,\ldots,K\}$ be the set of network tiers. In such a multi-tier network consisting of heterogeneous APs, the AP locations of the kth tier, where $k \in \mathcal{K}$, are usually modeled using a homogenous spatial PPP Φ_k of intensity λ_k [31], a model which we also follow in this paper. We will use the same notations given in Section II, with an added index $k \in \mathcal{K}$ when necessary to represent the parameters of an AP in the kth tier, *e.g.*, D_k, M_k and P_k represent the coverage radius, number of orthogonal beams, and the transmit power per beam for an AP in tier k, respectively.

Consider an AP in tier $k \in \mathcal{K}$ located at the origin $o \in \Phi_k$ and an MU i located at $u_{k,i} \in C_{D_k}$ that communicates with the AP located at o. Here, C_{D_k} represents the disk centered at the origin with a radius D_k. Note that the coverage radius will be different among tiers, with macro APs having large coverage radii and the femto and pico APs having relatively small coverage radii. The received SINR value $\gamma_{o,u_{k,i},m}$ of the MU located at $u_{k,i}$ corresponding to beam m transmitted from the AP at o is given by

$$\gamma_{o,u_{k,i},m} = \frac{g_{k,i} P_k X_{o,u_{k,i},m}}{I_{o,u_{k,i},m}}, \tag{9}$$

where

$$I_{o,u_{k,i},m} = 1 + g_{k,i} P_k I_o + \sum_{y_k\in\Phi_k\setminus\{o\}} G(\|u_{k,i}-y_k\|) P_k I_{y_k} + \sum_{j=1,j\neq k}^{K} \sum_{y_j\in\Phi_j} P_j G(\|u_{k,i}-y_j\|) I_{y_j},$$

1536-1276 (c) 2015 IEEE. Personal use is permitted, but republication/redistribution requires IEEE permission. See http://www.ieee.org/publications_standards/publications/rights/index.html for more information.

This article has been accepted for publication in a future issue of this journal, but has not been fully edited. Content may change prior to final publication. Citation information: DOI 10.1109/TWC.2016.2527650, IEEE Transactions on Wireless Communications

$g_{k,i}$ is the intra-AP path loss value of MU i at $u_{k,i}$, $X_{o,u_{k,i},m} = |\boldsymbol{h}_{o,u_{k,i}}^{\top}\boldsymbol{b}_{o,m}|^2$, $I_o = \sum_{l=1,l\neq m}^{M_k} X_{o,u_{k,i},l}$, and $I_{y_j} = \sum_{l=1}^{M_j} X_{y_j,u_{k,i},l}$ for $j \in \mathcal{K}$. The instantaneous rate on beam m transmitted from the AP at o (measured in terms of nats/s/Hz) can be written as

$$\text{rate}_m = \log\left(1 + \max_{1\leq i\leq N_k} \gamma_{o,u_{k,i},m}\right), \tag{10}$$

where N_k is the number of home MUs within the coverage area of the tier-k test AP at the origin.

Note that compared to (3), (9) has an extra term $\sum_{j=1,j\neq k}^{K}\sum_{y_j\in\Phi_j} P_j G(\|u_{k,i}-y_j\|)I_{y_j}$ in the denominator that represents the effect of the interference from the APs in all other tiers except tier $k \in \mathcal{K}$. We call this term inter-tier interference. As is done above, it can be shown that I_{y_j} is distributed according to the gamma distribution, *i.e.*, $I_{y_j} \sim \Gamma(M_j, 1)$. Thus, inter-tier interference can be dealt with by following the same approach used to deal with the inter-AP interference in the single tier scenario. To this end, the conditional distribution of beam SINR values in Lemma 1 can be easily extended to the case of heterogeneous networks with K-tiers. That is, for a given realization of the interfering APs $\Phi_o^! = \{\Phi_k \setminus \{o\}\} \bigcup \bigcup_{j=1,j\neq k}^{K} \Phi_j$, the distribution of the SINR on a beam of the MU at $u_{k,i}$ and communicating with the AP at $o \in \Phi_k$ is given by

$$F_{u_{k,i}}\left(t|\Phi_o^!\right) = 1 - \frac{\exp\left(\frac{-t}{g_{k,i}P_k}\right)}{(t+1)^{M_k-1}} \prod_{y\in\Phi_k\setminus\{o\}} \frac{g_{k,i}^{M_k}}{\left(g_{k,i}+tG(\|u_{k,i}-y\|)\right)^{M_k}} \times \prod_{j=1,j\neq k}^{K}\prod_{z\in\Phi_j} \frac{\left(P_k g_{k,i}\right)^{M_j}}{\left(g_{k,i}P_k + tP_jG(\|u_{k,i}-z\|)\right)^{M_j}}. \tag{11}$$

To obtain this expression, we have fixed the locations of all APs (except the AP at o) in tier k and the locations of those other APs causing inter-tier interference. Compared to (5), (11) also contains an extra term, which is due to the effect of inter-tier interference.

As discussed in Section III, an expression for the distribution of the maximum beam SINR is hard to obtain. Thus, we provide two approximated distributions below. The expression in (11) can be used to obtain these approximations by following similar concepts/steps to the ones used in the single tier analysis in Section III. For the first approximation, we will assume that the random variables representing inter-AP and inter-tier interference are independent among the MUs connected to a particular AP. With this assumption, we extend Theorem 1 to its respective K-tier version as follows. The proof of this theorem is skipped to avoid repetitions.

Theorem 3: Consider an AP belonging to tier $k \in \mathcal{K}$ and communicating with N_k MUs having intra-AP path loss values $\{g_{k,i}\}_{i=1}^{N_k}$. Under the independent inter-AP and inter-tier interference assumption, the CDF of the maximum SINR on a beam transmitted by the AP can be approximated by

$$F_{\text{ind},k}^{\star}(t) = \prod_{i=1}^{N_k}\left[1 - \frac{\exp\left(-q_{1,k,i}(t)\right)}{(t+1)^{M_k-1}}\right],$$

where

$$q_{1,k,i}(t) = \frac{t}{g_{k,i}P_k} + \sum_{j=1}^{K}\sum_{m=0}^{M_j-1}\int_0^{\infty} \frac{\pi\lambda_j P_j \left(P_k g_{k,i}\right)^m G(\sqrt{r})t}{\left(tP_jG(\sqrt{r}) + g_{k,i}P_k\right)^{m+1}} dr.$$

We will obtain our second approximation on the maximum beam SINR distribution by assuming that inter-AP and inter-tier interference random variables are perfectly correlated among the MUs connected to the same home AP. This assumption again makes the conditional beam SINR values (conditioned on the interfering AP locations) among the MUs connected to the same home AP independent. In the following theorem, we extend Theorem 2 to its respective K-tier version.

Theorem 4: Consider an AP belonging to tier $k \in \mathcal{K}$ and communicating with N_k MUs having intra-AP path loss values $\{g_{k,i}\}_{i=1}^{N_k}$. Under the perfectly correlated inter-AP and inter-tier interference assumption, the CDF of the maximum SINR on a beam transmitted by the AP can be approximated by

$$F_{\text{cor},k}^{\star}(t) = \sum_{\mathcal{S}\subseteq\{1,\ldots,N\}} \frac{(-1)^{|\mathcal{S}|}}{(1+t)^{|\mathcal{S}|(M_k-1)}} \exp\left(-q_{2,k}(t,\mathcal{S})\right),$$

where

$$q_{2,k}(t,\mathcal{S}) = \sum_{i\in\mathcal{S}} \frac{t}{g_i P} + \sum_{j=1}^{K} \pi\lambda_j \int_0^{\infty}\left(1 - \prod_{i\in\mathcal{S}} \frac{\left(P_k g_{k,i}\right)^{M_j}}{\left(g_{k,i}P_k + tP_jG(\sqrt{r})\right)^{M_j}}\right) dr.$$

The proof of this theorem is also skipped to avoid repetitions.

Next, similar to what was done for the single tier scenario, we will further simplify the results in Theorems 3 and 4 by assuming that the MUs are equidistant from the serving AP. The results for the independent inter-AP and inter-tier interference case and perfectly correlated inter-AP and inter-tier interference case are presented in the following two corollaries.

Corollary 3: Consider an AP belonging to tier $k \in \mathcal{K}$ and communicating with N_k equidistant MUs having the same intra-AP path loss value g_k. Under the independent inter-AP and inter-tier interference assumption, the CDF of the maximum SINR on a beam transmitted by the AP can be approximated by

$$F_{\text{ind},k}^{\star}(t) = \left[1 - \frac{\exp\left(-q_{3,k}(t)\right)}{(t+1)^{M_k-1}}\right]^{N_k},$$

where

$$q_{3,k}(t) = \frac{t}{g_k P_k} + \sum_{j=1}^{K}\sum_{m=0}^{M_j-1}\int_0^{\infty} \frac{\pi\lambda_j P_j \left(P_k g_k\right)^m G(\sqrt{r})t}{\left(tP_jG(\sqrt{r}) + g_k P_k\right)^{m+1}} dr.$$

Corollary 4: Consider an AP belonging to tier $k \in \mathcal{K}$ and communicating with N_k equidistant MUs having the same intra-AP path loss value g_k. Under the perfectly correlated inter-AP and inter-tier interference assumption, the CDF of the maximum SINR on a beam transmitted by the AP can be approximated by

$$F_{\text{cor},k}^{\star}(t) = 1 + \sum_{i=1}^{N_k} \frac{\binom{N_k}{i}(-1)^i \exp\left(-q_{2,k,i}(t)\right)}{(1+t)^{i(M_k-1)}},$$

1536-1276 (c) 2015 IEEE. Personal use is permitted, but republication/redistribution requires IEEE permission. See http://www.ieee.org/publications_standards/publications/rights/index.html for more information.

This article has been accepted for publication in a future issue of this journal, but has not been fully edited. Content may change prior to final publication. Citation information: DOI 10.1109/TWC.2016.2527650, IEEE Transactions on Wireless Communications

where

$$q_{2,k,i}(t)=\frac{it}{g_kP_k}+\sum_{j=1}^{K}\sum_{m=0}^{iM_j-1}\int_0^{\infty}\frac{\pi\lambda_jP_j\left(P_kg_k\right)^m G(\sqrt{r})t}{\left(tP_jG(\sqrt{r})+g_kP_k\right)^{m+1}}dr.$$

V. Extension of results for random MU locations

Note that we have assumed that the intra-AP path loss values are fixed positive real numbers in the previous sections. This is done to ensure clarity in the results in Theorems 1 and 2. However, according to conventional assumptions when stochastic geometry is applied to model wireless networks, both APs and MU locations are assumed to be subject to PPPs, albeit with different intensities. In this section, we will discuss how the results above can be extended to a scenario where both AP locations and MU locations are random. To this end, consider that the set of MUs communicating with a particular home AP is distributed over the coverage area of this AP according to a PPP. More specifically the set of MUs communicating with the AP at $o\in\Phi$ is distributed over the disk centered at o with radius D according to a PPP $\Phi_{\mathrm{MU,o}}$ of intensity λ_{MU}. This means that the number of MUs inside the coverage area N is a Poisson distributed random variable with mean $\lambda_{\mathrm{MU}}\pi D^2$, and all MUs are uniformly distributed over the coverage area given a particular realization of N. Therefore, the intra-AP path loss values are now random, and they are governed by a path loss model $G_{\mathrm{MU}}(r)$, where r is the distance between an MU and its home AP. We call G_{MU} the intra-AP path loss model. Similar to G, G_{MU} is general and it can be any function that is continuous, positive, non-increasing, and $G_{\mathrm{MU}}(r)=O\left(r^{-\alpha}\right)$ as r grows large for some $\alpha>2$. Note that the intra-AP path loss values will be identically distributed among a set of MUs communicating with a particular home AP. Since the MU locations are modeled using a PPP, and since G_{MU} is non-increasing, the CDF of the intra-AP path loss of an MU can be written as

$$\mathcal{G}_{\mathrm{MU}}(g)=1-\left[\frac{G_{\mathrm{MU}}^{-1}(g)}{D}\right]^2.$$

Here, we define $G_{\mathrm{MU}}^{-1}(g)$ as $G_{\mathrm{MU}}^{-1}(g)=\inf\left\{r:G_{\mathrm{MU}}(r)\leq g\right\}$.

In this context, the results in Theorems 1 and 2 can be considered as the CDFs of the maximum SINR on a beam conditioned on N and $\boldsymbol{g}=\{g_i\}_{i=1}^{N}$, *i.e.*, $F_{\mathrm{ind}}^{\star}(t|\boldsymbol{g},N)$ and $F_{\mathrm{cor}}^{\star}(t|\boldsymbol{g},N)$, where g_i's are now independent random variables distributed according to the CDF derived above. The distribution of the maximum SINR on a beam can be obtained by averaging over the location process of the MUs. To this end, averaging over the i.i.d. intra-AP path loss values gives us $F_{\mathrm{ind}}^{\star}(t|N)$ and $F_{\mathrm{cor}}^{\star}(t|N)$. Similarly, by observing that $\mathsf{Pr}\left\{N=n\right\}=\left[\mathrm{e}^{-\lambda_{\mathrm{MU}}\pi D^2}\left(\lambda_{\mathrm{MU}}\pi D^2\right)^n\right]/n!$, we can remove the condition on the number of MUs, and obtain the distribution of the maximum SINR on a beam. Although the idea of unconditioning the expressions in Theorems 1 and 2 over $\boldsymbol{g}$ and N is rather straightforward, the unconditioning does not lead to any simplification of the expressions. In fact, it further complicates them. Therefore, without formally presenting the results, we just discuss the idea of extending our results to a scenario where the MU locations are random. A similar approach can also be used to extend the results in Theorems 3 and 4 to a scenario where the MU locations are random.

VI. Applications for Specific Path Loss Models

The results above are presented for general path loss models. In this section, we apply our results to two well known path loss models, and in Section VII, the resulting expressions will be used to provide some further insights, and concrete examples illustrating the applications of the derived results, using numerical evaluations. For the applications, we will only focus on the results derived under the equidistant MU assumption in Corollaries 1, 2, 3 and 4 as they can be much effectively and easily used to provide further insights on the results, and to illustrate the validity of the two approximations (independent and perfectly correlated) for different network settings. We will again start with the single tier scenario. To this end, we observe that only the integral expression appearing in both Corollaries 1 and 2 depends on the functional form of the path loss model, which is given here again as

$$Q_m(t)=\int_0^{\infty}\frac{\pi\lambda tg^mG(\sqrt{r})}{\left(tG(\sqrt{r})+g\right)^{m+1}}dr. \tag{12}$$

Thus, it will be enough to simplify this integral expression further to understand the effect of the specific functional form of the path loss model on the maximum beam SINR distribution. To this end, we will use two commonly used path loss models in the literature. The first one is a bounded path loss model while the second one is an unbounded path loss model. For the bounded path loss model, the path loss function G takes the functional form of $G(r)=\left(1+r^{\alpha}\right)^{-1}$, where $\alpha>2$ (*e.g.*, see [10], [32], [33]). This bounded path loss model is also used in our numerical evaluations to illustrate network performance figures. For the unbounded path loss model, we use the classical unbounded path loss function $G(r)=r^{-\alpha}$, where $\alpha>2$ (*e.g.*, see [25], [31], [34]), which is the most commonly used path loss model in the literature. Our results simplifying the integral expression in (12) for these specific selections of path loss models are given in the following corollary.

Corollary 5: For the path loss model taking the form $G(r)=r^{-\alpha}$ for $\alpha>2$, $Q_m(t)$ in (12) can be written as

$$Q_m(t)=\binom{m+\frac{2}{\alpha}-1}{m}\frac{2\lambda\pi^2}{\alpha}\left(\frac{t}{g}\right)^{\frac{2}{\alpha}}\csc\left(\frac{2\pi}{\alpha}\right), \tag{13}$$

and for $G(r)=\left(1+r^{\alpha}\right)^{-1}$, where $\alpha>2$, it can be written as

$$Q_m(t)=\frac{2\lambda\pi^2t}{\alpha g}\csc\left(\frac{2\pi}{\alpha}\right)\times{}_2F_1\left(m+1,1-\frac{2}{\alpha};1;-\frac{t}{g}\right), \tag{14}$$

where ${}_2F_1$ represents the Gauss hypergeometric function [35].

Proof: For $G(r)=r^{-\alpha}$, $Q_m(t)$ in (12) can be written as

$$Q_m(t)=\pi\lambda\left(\frac{g}{t}\right)^m\int_0^{\infty}\frac{r^{\frac{\alpha m}{2}}}{\left(gr^{\frac{\alpha}{2}}/t+1\right)^{m+1}}dr.$$

Making a variable change $r^{\frac{\alpha}{2}}=v$ and using the techniques introduced in [35] for further simplification leads to (13). Since

1536-1276 (c) 2015 IEEE. Personal use is permitted, but republication/redistribution requires IEEE permission. See http://www.ieee.org/publications_standards/publications/rights/index.html for more information.

This article has been accepted for publication in a future issue of this journal, but has not been fully edited. Content may change prior to final publication. Citation information: DOI 10.1109/TWC.2016.2527650, IEEE Transactions on Wireless Communications

the proof of (14) follows along the similar lines, we skip it to avoid repetitions. ■

Results for the heterogeneous case can be obtained by focusing on

$$Q_{m,j}(t) = \int_0^\infty \frac{\pi \lambda_j P_j \left(P_k g_k\right)^m G(\sqrt{r}) t}{\left(t P_j G(\sqrt{r}) + g_k P_k\right)^{m+1}} dr,$$

which is the integral expression appearing in both Corollaries 3 and 4 that depends on the functional form of the path loss model. It is not hard to see that taking the results in Corollary 5 and replacing λ with λ_j and g with $g_k P_k / P_j$ will give us the required extension to the heterogeneous AP scenario, *i.e.*, $Q_{m,j}$ for $G(r) = r^{-\alpha}$ and $G(r) = (1 + r^\alpha)^{-1}$, where $\alpha > 2$. We do not formally present these results to avoid repetition.

By focusing on the bounded path loss model $G(r) = (1 + r^\alpha)^{-1}$ and the respective maximum beam SINR distributions given through Corollaries 1 2 and 5 for this path loss model, we will provide some numerical evaluations in the next section to illustrate the applications of maximum beam SINR distribution approximations derived above.

VII. Numerical Evaluations

In this section, we will demonstrate the utility of analytical results obtained for general network models by focusing on specific communication scenarios through numerical evaluations. We only focus on the single tier networks to keep the notations simpler. However, the same qualitative conclusions continue to hold for other selections of the system parameters as well as HetNet scenarios. We assume that the MUs are equidistant from the home AP and without any loss of generality, we assume that the MUs are located at the edge of the coverage area. That is, the distance to the home MUs from an AP is D, which is the radius of the coverage area. To this end, we consider four separate communication scenarios differing from each other with respect to D and the average number of interferers per coverage area μ, *i.e.*, $\mu = \lambda \pi D^2$. All other network parameters are kept constant as $M = 2$, $N = 20$ and $\alpha = 4$.

We set the intra-AP path-loss value to $g = (1 + D^\alpha)^{-1}$ and assume that the transmit powers per beam are controlled such that all beams are received with an average *unit* power, *i.e.*, $Pg = 1$. We note this assumption implies that increasing D results in APs transmitting at higher power levels, and as a result, MUs have the same received SNR in all four communication scenarios studied. This is necessary to have a fair comparison among different communication scenarios studied in our numerical evaluations. We note that, without such a normalization, our approximation results automatically become more accurate with increasing coverage radii as increasing the communication distance makes the received SINR CDFs more concentrated around small values with short dynamic ranges.

For the first communication scenario, we set $D = 0.5$ and $\mu = 0.05$. These selections of network parameters mean that the network model of interest consists of sparsely distributed APs having small coverage radii (in terms of the inter-AP interference power levels) over the plane. Our approximation

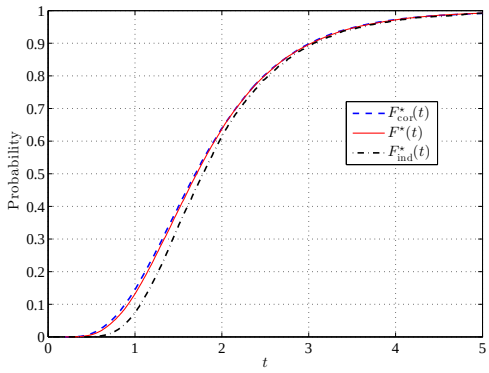

(a) $D = 0.5$

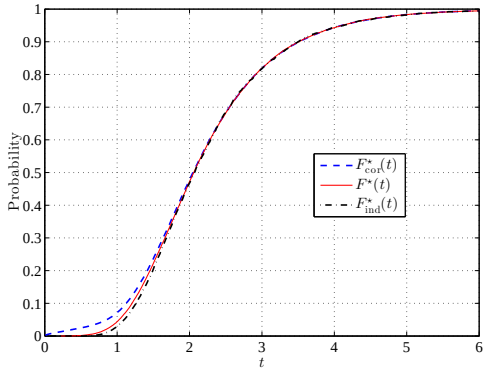

(b) $D = 5$

Fig. 2. The behavior of the CDFs for sparse networks with $\mu = 0.05$.

results (including both independent and perfectly correlated inter-AP interference cases) for the CDF of received SINR values at MUs are illustrated in Fig. 2(a), along with the realistically simulated CDF of the received SINR values. On the other hand, Fig. 2(b) demonstrates the approximation results for a network consisting of APs with relatively larger coverage radii but again sparsely distributed in terms of inter-AP interference power levels (*i.e.*, $D = 5$ and $\mu = 0.05$) when compared with the network model used to sketch Fig. 2(a).

In Fig. 3, we focus on network models that are highly dense in terms of inter-AP interference. In particular, Fig. 3(a) demonstrates the SINR CDFs (both approximated and realistically simulated ones) for a network consisting of APs with small coverage radii (*i.e.*, $D = 0.5$) and large inter-AP interference power levels (*i.e.*, $\mu = 1$), whereas Fig. 3(b) gives analogous results for a network consisting of larger coverage radii (*i.e.*, $D = 5$) and having the same inter-AP interference power level with the network in Fig. 3(a). Next, we compare and contrast the results obtained in Figs. 2(a) and 3(a).

We observe from Figs. 2(a) and 3(a) that when the coverage radius is small, the perfectly correlated inter-AP interference approximation gives rise to a close match to the actual SINR in both sparse and dense networks. This observation provides a quantitative justification for the intuition that led us to propose the perfectly correlated inter-AP interference approximation for the maximum beam SINR distribution in Section III. That is, it is anticipated that the MUs communicating with AP with small coverage radius are located close to each other,

1536-1276 (c) 2015 IEEE. Personal use is permitted, but republication/redistribution requires IEEE permission. See http://www.ieee.org/publications_standards/publications/rights/index.html for more information.

This article has been accepted for publication in a future issue of this journal, but has not been fully edited. Content may change prior to final publication. Citation information: DOI 10.1109/TWC.2016.2527650, IEEE Transactions on Wireless Communications

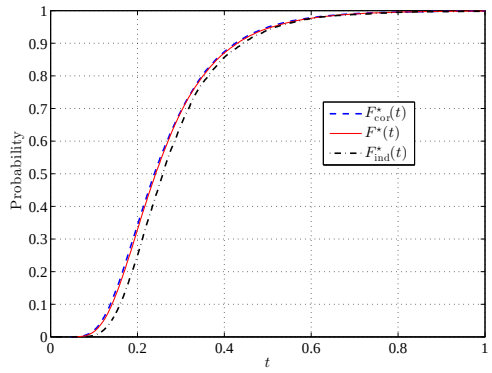

(a) $D = 0.5$

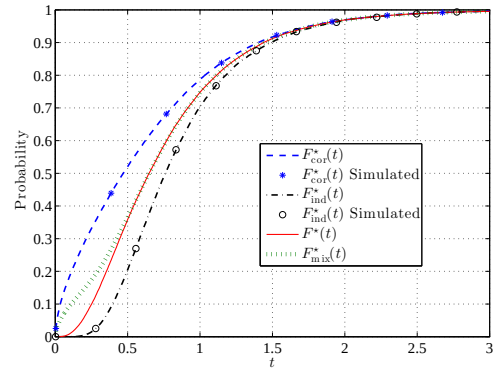

(b) $D = 5$

Fig. 3. The behavior of the CDFs for dense networks with $\mu = 1$.

and the spatial correlation coefficient of inter-AP interference increases to one for small distances [27]. Large spatial correlation implies that all MUs experience more or less the same inter-AP interference value, which leads to the above observed phenomenon of close match between the actual CDF and its perfectly correlated inter-AP interference approximation.

On the other hand, we observe in Fig. 2(b) that the independent inter-AP interference approximation performs better for sparse networks when the coverage radius is large. This observation is also expected because MUs are located far away from each other when the coverage radius is large, and the spatial correlation coefficient of inter-AP interference diminishes to zero for large distances [27]. However, the auto-correlation function of the spatial interference field increases with interfering AP density, and therefore how large the coverage radius should be to make interference values uncorrelated depends also on the network density. In particular, we see in Fig. 3(b) that when the coverage radius is large and the network is dense, the independent inter-AP interference approximation does not perform well, neither does the perfectly correlated inter-AP interference approximation. For such cases where both of the proposed SINR approximations do not perform well, a plausible approach is to use a convex combination of the two proposed SINR distribution approximations to better fit the actual maximum beam SINR CDF.

To illustrate this point more clearly, we provide an example combination of $F^{\star}_{\mathrm{cor}}(t)$ and $F^{\star}_{\mathrm{ind}}(t)$ as $F^{\star}_{\mathrm{mix}}(t) = 0.5F^{\star}_{\mathrm{cor}}(t)+0.5F^{\star}_{\mathrm{ind}}(t)$ in Fig. 3(b). In this particular example, we set the mixing coefficient to 0.5, and an optimal selection of this coefficient relies upon the correlation between the SINR values considered for choosing the best MU with the maximum SINR for downlink communication at each beam. As seen in this figure, $F^{\star}_{\mathrm{mix}}(t)$ fits to the maximum beam SINR distribution more closely for most values of interference levels. In fact, the approach proposed above is just a heuristic one. For a more rigorous treatment of this problem, one first needs to determine a metric to measure the distance between $F^{\star}$ and $F^{\star}_{\mathrm{mix}}$ such as the Kullback-Leibler divergence or the Kolmogorov-Smirnov distance. Then, the mixing coefficient that minimizes the distance between two distributions can be found either numerically or analytically, whichever more convenient to carry out, for given values of D and λ. This process can be repeated initially for all possible pairs of λ and D, and the respective optimal mixing coefficients can be tabulated. Then, for any given D and λ, the system implementer will readily have access to the optimal mixing coefficient, or at least a near optimal mixing coefficient given that the exact D or λ is not to be found in the table. A final remark is that we have also provided simulation results to validate the expressions obtained for the two approximations in Fig. 3(b). We have simulated over a 120×120 rectangular area, and we have considered 350000 realizations of the Poisson process. For clarity, we have omitted these simulation results in Figs. 2(a), 2(b) and 3(a).

It is important to note that $F^{\star}_{\mathrm{ind}}$ and $F^{\star}_{\mathrm{cor}}$ do in fact provide a *lower* bound and an *upper* bound to the actual maximum beam SINR distribution in Figs. 2 and 3, respectively. This is a rather intuitive observation. For the perfectly correlated inter-AP interference approximation, we assume the collection of distances/path loss values between an MU and its interfering APs to be the same for all MUs connected to a particular AP. For the independent inter-AP interference approximation, on the other hand, we assume that the collection of distances/path loss values between an MU and its interfering APs consists of independent random variables among the MUs. Thus, the beam SINR values vary more significantly from one MU to another one in the independent inter-AP interference case than the variances of those in the perfectly correlated inter-AP interference case.

The maximization operation to choose the best MU achieving the highest rate on each beam (*i.e.*, see (4)) benefits from such a higher variance in the independent inter-AP interference case. To put in other words, we can better exploit multiuser diversity gains when the correlation structure of the beam SINR values leads to larger dynamic ranges for the maximum beam SINR CDF [36], which is the case in the independent inter-AP interference approximation. In the actual scenario, the inter-AP interference will neither be perfectly correlated nor independent. Therefore, it will lie in the middle ground between these two extreme cases, and that's why we observe $F^{\star}_{\mathrm{ind}}$ and $F^{\star}_{\mathrm{cor}}$ as lower and upper bounds to the realistically simulated CDF of the maximum beam SINR in above figures.

We can use Figs. 2 and 3 to get insights into the heterogeneous AP scenario as well. In general, the heterogeneous AP scenario will lead to denser deployment of the APs due to interfering APs in different tiers. Therefore, Fig. 3 will be

1536-1276 (c) 2015 IEEE. Personal use is permitted, but republication/redistribution requires IEEE permission. See http://www.ieee.org/publications_standards/publications/rights/index.html for more information.

This article has been accepted for publication in a future issue of this journal, but has not been fully edited. Content may change prior to final publication. Citation information: DOI 10.1109/TWC.2016.2527650, IEEE Transactions on Wireless Communications

of more relevance. This figure tells us that when the coverage radius is small, the perfectly correlated scenario will be a better fit, and when the coverage radius is large, the mixing technique will provide a better fit. This means, for pico and femto APs, the approximation obtained using the perfect correlation assumption in Theorem 4 and Corollary 4 will be better suited for performance evaluation. On the other hand, the mixing technique will be better suited for performance analysis of macro APs and other APs having a large coverage radius. Alternatively, we can numerically evaluate the results obtained in Section VI with regards to the heterogeneous AP scenario, and obtain similar insights. However, we are skipping these to avoid repetition of figures that look similar to each other.

The utility of our CDF approximation results becomes more prominent when we consider obtaining performance bounds for Poisson wireless networks operating according to OBF. In particular, these approximations can be used to analyze some important performance measures such as outage probability and ergodic capacity for multi-AP OBF systems. Starting with outage probability calculations, we consider fixed rate communication on each beam for delay sensitive traffic. In this case, the beam outage probability becomes a relevant metric to measure the system performance. Considering an AP located at the origin and a particular beam, say beam m, without loss of generality due to symmetry among beams and Slivnyak's Theorem, the beam outage probability can be written as

$$\begin{aligned}\mathsf{Pr}\left(\text{Beam Outage}\right) &= \mathsf{Pr}\left\{\log\left(1+\max_{1\leq i\leq N}\gamma_{o,i,m}\right)\leq t\right\}\\ &= F^{\star}\left(\mathrm{e}^{t}-1\right)\end{aligned}$$

for a target data rate t. If an outage event occurs at a beam, this beam cannot be scheduled for reliable communication until it faces better channel states. Using our independent and perfectly correlated inter-AP interference approximation results, we can upper and lower bound $\mathsf{Pr}\left(\text{Beam Outage}\right)$ as

$$F^{\star}_{\text{ind}}\left(\mathrm{e}^{t}-1\right)\leq \mathsf{Pr}\left(\text{Beam Outage}\right)\leq F^{\star}_{\text{cor}}\left(\mathrm{e}^{t}-1\right),$$

which are quite tight bounds, especially for target rates greater than 1 [nats/s/Hz] as depicted in Fig. 4. Further, these bounds can also be utilized to estimate the outage capacity of a multi-AP OBF communication system, defined as the supremum of target rates that can be sustained by each beam without exceeding a given threshold level for outage probability.[3] In Fig. 4, we only demonstrate beam outage probabilities for sparsely distributed OBF Poisson wireless networks consisting of APs with small coverage radii. The other three scenarios considered above to illustrate our approximation results for the distribution of the maximum beam SINR values have been omitted to avoid repetitions.

The same approach can also be used to obtain ergodic data rates for multi-AP OBF communication systems. Considering an AP located at the origin, we can write the aggregate average data rate that can be sustained to support reliable communication of delay insensitive data as

[3]A similar calculation was carried out for single AP OBF communication systems in [10].

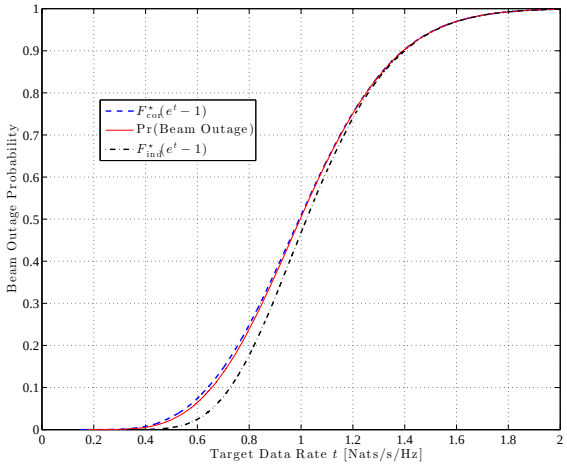

Fig. 4. Beam outage probability for $D=0.5$ and $\mu=0.05$.

TABLE I
AVERAGE ACHIEVABLE RATE OF AN AP PER BEAM (NATS/S/HZ). ($M=2$, $N=20$ AND $\alpha=4$.)

Interference	$D=0.5$ $\mu=0.05$	$D=0.5$ $\mu=1$	$D=5$ $\mu=0.05$	$D=5$ $\mu=1$
Independent	1.0444	0.2463	1.1487	0.5990
Actual	1.0138	0.2345	1.1387	0.5378
Perfectly Correlated	1.0082	0.2323	1.1189	0.4291
Mix	1.0208	0.2401	1.1239	0.5101

$$\begin{aligned}R_{\text{ergodic}} &= \mathsf{E}\left[\sum_{m=1}^{M}\log\left(1+\max_{1\leq i\leq N}\gamma_{o,i,m}\right)\right]\\ &= M\int_{0}^{\infty}\mathsf{Pr}\left\{\log\left(1+\max_{1\leq i\leq N}\gamma_{o,i,m}\right)>t\right\}dt\\ &= M\int_{0}^{\infty}\left(1-F^{\star}\left(\mathrm{e}^{t}-1\right)\right)dt,\end{aligned}$$

where we used the property that $\log\left(1+\max_{1\leq i\leq N}\gamma_{o,i,m}\right)$ is always a positive number to write the first identity. Hence, R_{ergodic} can be upper and lower bounded as

$$M\int_{0}^{\infty}\left(1-F^{\star}_{\text{cor}}\left(\mathrm{e}^{t}-1\right)\right)dt\leq R_{\text{ergodic}}\leq M\int_{0}^{\infty}\left(1-F^{\star}_{\text{ind}}\left(\mathrm{e}^{t}-1\right)\right)dt.$$

Table I tabulates the average achievable rate of an AP per beam for the four scenarios considered in Figs. 2 and 3. In this table, we also provide average achievable data rates obtained through using the mixing approach to approximate the maximum beam SINR distribution with the mixing coefficient 0.5, *i.e.*, $F^{\star}(t)\approx F^{\star}_{\text{mix}}(t)=0.5F^{\star}_{\text{cor}}(t)+0.5F^{\star}_{\text{ind}}(t)$. We recall that the strategy of approximating $F^{\star}(t)$ through mixing of $F^{\star}_{\text{cor}}(t)$ and $F^{\star}_{\text{ind}}(t)$ works fine when neither the independent inter-AP interference approximation and nor the perfectly correlated inter-AP interference approximation comes close enough to $F^{\star}$. Indeed, from Table I, it can be seen that both independent inter-AP interference approximation and perfectly correlated inter-AP interference approximation very well match to the

1536-1276 (c) 2015 IEEE. Personal use is permitted, but republication/redistribution requires IEEE permission. See http://www.ieee.org/publications_standards/publications/rights/index.html for more information.

This article has been accepted for publication in a future issue of this journal, but has not been fully edited. Content may change prior to final publication. Citation information: DOI 10.1109/TWC.2016.2527650, IEEE Transactions on Wireless Communications

realistically simulated ergodic data rates in the first three cases when the network either contains APs with small coverage radii or it is sparse in terms of inter-AP interference values. On the other hand, the approximated data rates obtained by using $F^{\star}_{\text{mix}}(t)$ match to the actual data rates much better when the network contains APs with large coverage radii and large inter-AP interference levels. The same explanations regarding the suitability of each approximation also hold for outage probabilities, which we do not restate here to avoid repetitions.

VIII. Conclusions

In this paper, we have introduced a model to study both single tier and multi-tier multi-AP opportunistic communication systems, in which wireless access point locations are modeled using a Poisson point process, and that operate according to the classical opportunistic beamforming framework. The received signals at MUs are impaired by both fading and location dependent path loss. Considering a closed-access network, where each AP communicates with a multitude of non-equidistant MUs, and communication scheduled to the MU having the best SINR on each beam, we have focused on the distribution of the maximum beam SINR by using key tools from stochastic geometry. The SINR values at MUs are dependent on the point process characterizing the locations of the interfering wireless access points. Thus, obtaining an expression for the distribution of the maximum beam SINR becomes untractable due to the maximization of a set of correlated random variables. Towards the resolution of this complication, we have provided two tight distribution approximation results. The derived distribution approximation results have been validated through simulations and numerical evaluations. In particular, we have shown that for APs with small coverage radii, the approximation obtained by assuming perfect correlation gives rise to a close match to the actual case in both sparse and dense networks. On the other hand, the approximation obtained by assuming independent inter-AP interference performs better for sparse networks when the coverage radius is large. The utility of these distribution approximation results has also been illustrated by obtaining some important performance measures for multi-AP OBF communication systems such as beam outage probability and ergodic aggregate data rate per AP.

Appendix A
Distribution of the Maximum SINR on a Beam

A. Given Realization of AP Locations: Proof of Lemma 1

Let $I_{\text{sum}} = \sum_{y\in\Phi\setminus\{o\}} G(\|u_i - y\|)I_y$. We have

$$\mathsf{Pr}\left\{\gamma_{o,u_i,m} > t|\Phi_o^!\right\} = \mathsf{Pr}\left\{\frac{g_i X_{o,u_i,m}}{(P)^{-1}+ g_i I_o + I_{\text{sum}}} > t \middle| \Phi_o^!\right\}.$$

Then, by conditioning on I_o and $\{I_y\}_{y\in\Phi_o^!}$, and by using the fact that $X_{o,u_i,m}\sim\exp(1)$, we get

$$\begin{aligned}
&\mathsf{Pr}\left\{\gamma_{o,u_i,m} > t|\Phi_o^!\right\} \\
&\quad= \mathsf{E}_{I_o,I_y}\left[\exp\left(-tI_o - \frac{t}{g_i}I_{\text{sum}}\right)\middle|\Phi_o^!\right]\exp\left(\frac{-t}{g_i P}\right) \\
&\quad= \mathsf{E}_{I_o}\left[\mathrm{e}^{-tI_o}\right]\mathsf{E}_{I_y}\left[\mathrm{e}^{-\frac{t}{g_i}I_{\text{sum}}}\middle|\Phi_o^!\right]\exp\left(\frac{-t}{g_i P}\right). \quad (15)
\end{aligned}$$

Furthermore, since I_o is a $\Gamma(M-1,1)$ distributed random variable, we have

$$\mathsf{E}_{I_o}\left[\mathrm{e}^{-tI_o}\right] = \int_0^\infty \frac{\mathrm{e}^{-y(t+1)}y^{M-2}}{\Gamma(M-1)}dy = \frac{1}{(t+1)^{M-1}}. \quad (16)$$

Also note that $\{I_y\}_{y\in\Phi_o^!}$ form an i.i.d. collection of random variables with common distribution $\Gamma(M,1)$, hence we obtain

$$\begin{aligned}
\mathsf{E}_{I_y}\left[\mathrm{e}^{-\frac{t}{g_i}I_{\text{sum}}}\middle|\Phi_o^!\right] &= \prod_{y\in\Phi_o^!}\mathsf{E}_{I_y}\left[\mathrm{e}^{\frac{-tI_y G(\|u_i-y\|)}{g_i}}\right] \\
&= \prod_{y\in\Phi_o^!}\frac{g_i^M}{\left(g_i + tG(\|u_i-y\|)\right)^M} \quad (17)
\end{aligned}$$

after averaging over all $I_y, y\in\Phi_o^!$. Substituting (16) and (17) in (15) and considering $F_{u_i}\left(t|\Phi_o^!\right) = 1-\mathsf{Pr}\left\{\gamma_{o,u_i,m} > t|\Phi_o^!\right\}$ gives us (5), which completes the proof.

B. Independent Inter-AP Interference Approximation: Proof of Theorem 1

Note that $\Phi_o^!$ is a PPP of intensity λ on $\mathbb{R}^2$ since the reduced Palm distribution of a PPP is equal to the distribution of the PPP itself. Hence, by using the probability generating functionals for PPPs, and by changing the coordinates from Cartesian to polar and evaluating the resulting integration over the area of the interfering APs, we have

$$\begin{aligned}
&\mathsf{E}_{\Phi_o^!}\left[\prod_{y\in\Phi_o^!}\tilde{G}_i(t,u_i-y)\right] \\
&\quad= \exp\left(-\lambda\int_{\mathbb{R}^2}\left(1-\frac{g_i^M}{\left(g_i+tG(\|y\|)\right)^M}\right)dy\right) \\
&\quad= \exp\left(-\lambda\int_0^\infty\left(1-\frac{g_i^M}{\left(g_i+tG(v)\right)^M}\right)2\pi v dv\right) \\
&\quad= \exp\left(-\pi\lambda t\sum_{m=0}^{M-1}\int_0^\infty\frac{g_i^m G(\sqrt{r})}{\left(tG(\sqrt{r})+g_i\right)^{m+1}}dr\right) \quad (18)
\end{aligned}$$

after a variable change $v^2 = r$, some algebraic manipulations and factoring the binomials. Substituting the resulting expression in (7) gives us $F^{\star}_{\text{ind}}(t)$, which completes the proof.

1536-1276 (c) 2015 IEEE. Personal use is permitted, but republication/redistribution requires IEEE permission. See http://www.ieee.org/publications_standards/publications/rights/index.html for more information.

This article has been accepted for publication in a future issue of this journal, but has not been fully edited. Content may change prior to final publication. Citation information: DOI 10.1109/TWC.2016.2527650, IEEE Transactions on Wireless Communications

C. Perfectly Correlated Inter-AP Interference Approximation: Proof of Theorem 2

By using Lemma 2, $F^{\star}_{\mathrm{cor}}$ in (8) can be written as

$$\begin{aligned} &F^{\star}_{\mathrm{cor}}(t) \\ &= \mathsf{E}_{\Phi^!_o}\left[\sum_{\mathcal{S}\subseteq\{1,\ldots,N\}}(-1)^{|\mathcal{S}|}\prod_{i\in\mathcal{S}}\left(\frac{\exp\left(\frac{-t}{g_iP}\right)}{(t+1)^{M-1}}\prod_{y\in\Phi^!_o}\tilde{G}_i\left(t,y\right)\right)\right] \\ &= \sum_{\mathcal{S}\subseteq\{1,\ldots,N\}}\frac{(-1)^{|\mathcal{S}|}\prod_{i\in\mathcal{S}}\mathrm{e}^{\left(\frac{-t}{g_iP}\right)}}{(1+t)^{|\mathcal{S}|(M-1)}}\mathsf{E}_{\Phi^!_o}\left[\prod_{y\in\Phi^!_o}\prod_{i\in\mathcal{S}}\tilde{G}_i\left(t,y\right)\right]. \end{aligned}$$

Now, by resorting to similar steps used in the proof of Theorem 1 (*i.e.*, by using the probability generating functionals for PPPs, by changing the coordinates from Cartesian to polar and evaluating the resulting integration over the area of the interfering APs), we get

$$\begin{aligned} &\mathsf{E}_{\Phi^!_o}\left[\prod_{y\in\Phi^!_o}\prod_{i\in\mathcal{S}}\tilde{G}_i\left(t,y\right)\right] \\ &\quad= \exp\left(-\lambda\int_0^{\infty}\left(1-\prod_{i\in\mathcal{S}}\frac{g_i^M}{\left(g_i+tG(v)\right)^M}\right)2\pi v dv\right). \end{aligned}$$

A variable change $v^2 = r$ and some algebraic manipulations completes the proof.

D. Perfectly Correlated Inter-AP Interference Approximation: Proof of Corollary 2

If $g_i = g$ for all $i \in \{1,\ldots,N\}$, the result in Theorem 2 simplifies to

$$\begin{aligned} F^{\star}_{\mathrm{cor}}\left(t\right) = 1+\sum_{i=1}^{N}\frac{\binom{N}{i}\left(-1\right)^i\mathrm{e}^{-ti/gP}}{\left(1+t\right)^{i(M-1)}} \\ \times\,\mathsf{E}_{\Phi^!_o}\left[\prod_{y\in\Phi^!_o}\frac{g^{Mi}}{\left(g+tG(\|y\|)\right)^{Mi}}\right]. \end{aligned}$$

Directly from (18),

$$\begin{aligned} &\mathsf{E}_{\Phi^!_o}\left[\prod_{y\in\Phi^!_o}\frac{g^{Mi}}{\left(g+tG(\|y\|)\right)^{Mi}}\right] = \\ &\qquad\exp\left(-\pi\lambda t\sum_{m=0}^{Mi-1}\int_0^{\infty}\frac{g^mG(\sqrt{r})}{\left(g+tG(\sqrt{r})\right)^{m+1}}dr\right), \end{aligned}$$

which completes the proof.

REFERENCES

[1] M. Sharif and B. Hassibi, "On the capacity of MIMO broadcast channels with partial side information," *IEEE Trans. Inf. Theory*, vol. 51, pp. 506–522, Feb. 2005.

[2] M. Pugh and B. D. Rao, "Reduced feedback schemes using random beamforming in MIMO broadcast channels," *IEEE Trans. Signal Process.*, vol. 58, pp. 1821–1832, Mar. 2010.

[3] J. Diaz, O. Simeone, and Y. Bar-Ness, "Asymptotic analysis of reduced-feedback strategies for MIMO Gaussian broadcast channels," *IEEE Trans. Inf. Theory*, vol. 54, pp. 1308–1316, Mar. 2008.

[4] T. Samarasinghe, H. Inaltekin, and J. S. Evans, "Optimal selective feedback policies for opportunistic beamforming," *IEEE Trans. Inf. Theory*, vol. 59, pp. 2897–2913, May 2013.

[5] A. Bayesteh and A. Khandani, "Asymptotic analysis of the amount of CSI feedback in MIMO broadcast channels," *IEEE Trans. Inf. Theory*, vol. 58, pp. 1612–1629, Mar. 2012.

[6] M. Kountouris, D. Gesbert, and T. Salzer, "Enhanced multiuser random beamforming: Dealing with the not so large number of users case," *IEEE J. Sel. Areas Commun.*, vol. 26, pp. 1536–1545, Oct. 2008.

[7] R. Couillet, J. Hoydis, and M. Debbah, "Random beamforming over quasi-static and fading channels: A deterministic equivalent approach," *IEEE Trans. Inf. Theory*, vol. 58, pp. 6392–6425, Oct. 2012.

[8] T. Samarasinghe, H. Inaltekin, and J. S. Evans, "The feedback-capacity tradeoff for opportunistic beamforming under optimal user selection," *Performance Evaluation*, vol. 70, pp. 472–492, Jul. 2013.

[9] Y. Huang and B. D. Rao, "Random beamforming with heterogeneous users and selective feedback: Individual sum rate and individual scaling laws," *IEEE Trans. Wireless Commun.*, vol. 12, pp. 2080–2090, May 2013.

[10] T. Samarasinghe, H. Inaltekin, and J. S. Evans, "On the outage capacity of opportunistic beamforming with random user locations," *IEEE Trans. Commun.*, vol. 62, pp. 3015–3026, Aug. 2014.

[11] S.-H. Moon, S.-R. Lee, and I. Lee, "Sum-rate capacity of random beamforming for multi-antenna broadcast channels with other cell interference," *IEEE Trans. Wireless Commun.*, vol. 10, pp. 2440–2444, Aug. 2011.

[12] Y. Huang and B. D. Rao, "Reducing feedback requirements of the multiple weight opportunistic beamforming scheme via selective multiuser diversity," in *Proc. IEEE Vehicular Technology Conference*, Las Vegas, USA, pp. 1–5, Sep. 2013.

[13] H. D. Nguyen, R. Zhang, and H. T. Hui, "Multi-cell random beamforming: Achievable rate and degrees of freedom region," *IEEE Trans. Signal Process.*, vol. 61, pp. 3532–3544, May 2013.

[14] M. Wang, T. Samarasinghe, and J. S. Evans, "Transmission rank selection for opportunistic beamforming with quality of service constraints," in *Proc. International Conference on Communications*, Sydney, Australia, pp. 1904–1909, Jun. 2014.

[15] H. Ju and R. Zhang, "A novel mode switching scheme utilizing random beamforming for opportunistic energy harvesting," *IEEE Trans. Wireless Commun.*, vol. 13, pp. 2150–2162, Mar. 2014.

[16] J.-H. Li and H.-J. Su, "Opportunistic feedback reduction for multiuser MIMO broadcast channel with orthogonal beamforming," *IEEE Trans. Wireless Commun.*, vol. 13, pp. 1321–1333, Jan. 2014.

[17] Y. Xuezhi, J. Wei, and B. Vucetic, "A random beamforming technique for omnidirectional coverage in multiple-antenna systems," *IEEE Trans. Veh. Technol.*, vol. 62, pp. 1420–1425, Mar. 2013.

[18] C. Kim, S. Lee, and J. Lee, "SINR and throughput analysis for random beamforming systems with adaptive modulation," *IEEE Trans. Wireless Commun.*, vol. 12, pp. 1460–1471, Apr. 2013.

[19] J. Park, H. Lee, and S. Lee, "MIMO broadcast channels based on SINR feedback using a non-orthogonal beamforming matrix," *IEEE Trans. Commun.*, vol. 60, pp. 2534–2545, Sep. 2012.

[20] S. A. M. Xia, Y. Wu, "Non-orthogonal opportunistic beamforming: Performance analysis and implementation," *IEEE Trans. Wireless Commun.*, vol. 11, pp. 1424–1433, Apr. 2012.

[21] V. Chandrasekhar, M. Kountouris, and J. G. Andrews, "Coverage in multi-antenna two-tier networks," *IEEE Trans. Wireless Commun.*, vol. 8, pp. 5314–5327, Oct. 2009.

[22] K. Huang, J. G. Andrews, D. Guo, R. W. Heath, and R. A. V. Berry, "Spatial interference cancellation for multiantenna mobile ad hoc networks," *IEEE Trans. Inf. Theory*, vol. 58, pp. 1660–1676, Oct. 2012.

[23] M. Kountouris and J. G. Andrews, "Downlink SDMA with limited feedback in interference-limited wireless networks," *IEEE Trans. Wireless Commun.*, vol. 11, pp. 2730–2741, Aug. 2012.

[24] H. Dhillon, M. Kountouris, and J. G. Andrews, "Downlink MIMO HetNets: Modeling, ordering results and performance analysis.," *IEEE Trans. Wireless Commun.*, vol. 12, pp. 5208–5222, Oct. 2013.

[25] J. G. Andrews, F. Baccelli, and R. K. Ganti, "A tractable approach to coverage and rate in cellular networks," *IEEE Trans. Commun.*, vol. 59, pp. 3122–3134, Nov. 2011.

[26] J. G. Andrews, H. Claussen, M. Dohler, S. Rangan, and M. C. Reed, "Femtocells: Past, present, and future," *IEEE J. Sel. Areas Commun.*, vol. 30, pp. 497–508, Apr. 2012.

[27] M. Haenggi and R. K. Ganti, "Interference in large networks," *Foundations and Trends in Networking*, vol. 2, pp. 127–248, Nov. 2009.

1536-1276 (c) 2015 IEEE. Personal use is permitted, but republication/redistribution requires IEEE permission. See http://www.ieee.org/publications_standards/publications/rights/index.html for more information.

This article has been accepted for publication in a future issue of this journal, but has not been fully edited. Content may change prior to final publication. Citation information: DOI 10.1109/TWC.2016.2527650, IEEE Transactions on Wireless Communications

[28] M. Haenggi, J. G. Andrews, F. Baccelli, O. Dousse, and M. Franceschetti, "Stochastic geometry and random graphs for the analysis and design of wireless networks," *IEEE J. Sel. Areas Commun.*, vol. 27, pp. 1029–1046, Sep. 2009.

[29] M. Haenggi, *Stochastic Geometry for Wireless Networks*. Cambridge University Press, 2012.

[30] H. ElSawy, E. Hossain, and M. Haenggi, "Stochastic geometry for modeling, analysis, and design of multi-tier and cognitive cellular wireless networks: A survey," *IEEE Commun. Surveys and Tutorials*, vol. 15, pp. 996–1019, Jul. 2013.

[31] H. S. Dhillon, R. K. Ganti, F. Baccelli, and J. G. Andrews, "Modeling and analysis of K-tier downlink heterogeneous cellular networks," *IEEE J. Sel. Areas Commun.*, vol. 30, pp. 550–560, Apr. 2012.

[32] H. Inaltekin, M. Chiang, H. V. Poor, and S. B. Wicker, "On unbounded path-loss models: Effects of singularity on wireless network performance," *IEEE J. Sel. Areas Commun.*, vol. 27, pp. 1078–1092, Sep. 2009.

[33] T. Samarasinghe, H. Inaltekin, and J. S. Evans, "On optimal downlink coverage in Poisson cellular networks with power density constraints," *IEEE Trans. Commun.*, vol. 62, pp. 1382–1392, Feb. 2014.

[34] E. S. Sousa and J. A. Silvester, "Optimum transmission ranges in a direct sequence spread spectrum multihop packet radio network," *IEEE J. Sel. Areas Commun.*, vol. 8, pp. 762–771, Jun. 1990.

[35] I. Gradshteyn and I. Ryzhik, *Table of Integrals, Series, and Products*. 7th ed. Academic Press, 2007.

[36] D. N. C. Tse and P. Viswanath, *Fundamentals of Wireless Communications*. Cambridge University Press, 2005.

1536-1276 (c) 2015 IEEE. Personal use is permitted, but republication/redistribution requires IEEE permission. See http://www.ieee.org/publications_standards/publications/rights/index.html for more information.